



Dynamical Dependencies at Monthly and Interannual Time Scales in the Climate System: Study of the North Pacific and Atlantic Regions

STÉPHANE VANNITSEM 

X. SAN LIANG 

**Author affiliations can be found in the back matter of this article*

ORIGINAL RESEARCH
PAPER



STOCKHOLM
UNIVERSITY PRESS

ABSTRACT

The directional dependencies of different climate indices are explored using the Liang-Kleeman information flow in order to disentangle the influence of certain regions over the globe on the development of low-frequency variability of others. Seven key indices (the sea-surface temperature in El-Niño 3.4 region, the Atlantic Multidecadal Oscillation, the North Atlantic Oscillation, the North Pacific America pattern, the Arctic Oscillation, the Pacific Decadal Oscillation, the Tropical North Atlantic index), together with three local time series located in Western Europe (Belgium), are selected. The analysis is performed on time scales from a month to 5 years by using a sliding window as filtering procedure.

A few key new results on the remote influence emerge: (i) The Arctic Oscillation plays a key role at short time (monthly) scales on the dynamics of the North Pacific and North Atlantic; (ii) the North Atlantic Oscillation is playing a global role at long time scales (several years); (iii) the Pacific Decadal Oscillation is indeed slaved to other influences; (iv) the local observables over Western Europe influence the variability on the ocean basins on long time scales. These results further illustrate the power of the Liang-Kleeman information flow in disentangling the dynamical dependencies.

CORRESPONDING AUTHOR:

Stéphane Vannitsem

Royal Meteorological Institute of Belgium, Brussels, Belgium

Stephane.Vannitsem@meteo.be

KEYWORDS:

Dynamical dependencies; Information flow; Climate indices

TO CITE THIS ARTICLE:

Vannitsem, S and Liang, XS. 2022. Dynamical Dependencies at Monthly and Interannual Time Scales in the Climate System: Study of the North Pacific and Atlantic Regions. *Tellus A: Dynamic Meteorology and Oceanography*, 74(2022), 141–158. DOI: <https://doi.org/10.16993/tellusa.44>

1. INTRODUCTION

Long-term forecasting from seasonal-to-decadal time scales of the atmospheric evolution is based on the main hypothesis that there are low-frequency signals embedded in its dynamics either associated with an internal variability or with external interactions with the other components of the climate system. One key source of such low-frequency variability originates from the slow dynamics of the coupled ocean-atmosphere in the Tropical Pacific, e.g. Philander (1990); Alexander et al. (2002); Liu and Alexander (2007); Tsonis and Swanson (2012); Stan et al. (2017); Soulard et al. (2021). Other sources can also be at the origin of this low-frequency variability, like the local interaction between the ocean and the atmosphere in the extratropics, e.g. Mantua et al. (1997); Kravtsov et al. (2007); Gastineau et al. (2013); Vannitsem and Ghil (2017), or the interaction with the Polar regions (Wang et al., 2017). Disentangling the impact of the potential sources of low-frequency variability on the different regions all over the World are essential to properly address the limits of predictability.

Usually the analysis of the impact of a region on another is done through either teleconnection analysis based on correlation, e.g. Philander (1990), or by investigating the sensitivity of the climatology of a region in a climate model by forcing another key region, e.g. Johnson et al. (2020). These approaches, although useful, do not allow to disentangle the one-way or two-way interactions between remote regions. During the last decades, there were considerable efforts devoted to the development of approaches allowing to clarify the causality between different observables, see the recent reviews of Palus et al. (2018); Runge et al. (2019), and some applications to atmospheric and climate data, e.g. Mosedale et al. (2006); Wang et al. (2009); Tsonis et al. (2015); Vannitsem and Ekkelmans (2018); Vannitsem et al. (2019); Di Capua et al. (2020).

One very useful approach developed in Liang and Kleeman (2005) and Liang (2014a; 2016) is based on the rate of information flow in dynamical systems. Based on this theoretical background, Liang (2014b) developed a simple method to estimate the rate of information flow in 2-dimensional linear stochastic systems, and extended it to multi-variate linear stochastic systems, see Liang (2021). The latter development allows for an analysis of the multiple influences among a set of observables, and the construction of a dynamical dependence graph. This is the approach we will adopt in the present work to disentangle the influence of certain climate indices on the development of low-frequency variability on others.

We focus here on a set of indices that were produced to characterize the observed large scale dynamics of the atmosphere and the oceans from 1950 to 2020 at monthly time scale, and a set of local observables over Belgium (temperature, precipitation and insolation).

The latter are used to clarify the local role of large-scale features. As we will see there are surprising influences of the local observables on the global ones. The indices used are characterizing the slow dynamics over the North and Central Pacific and and the North and Central Atlantic.

In Section 2, the data used are briefly presented. Section 3 is then devoted to the description of the methodology adopted here. The results are then presented in Section 4, and finally Section 5 is summarizing the results.

2. DATA

The current analysis is performed on a set of key indices that were found to show low-frequency variability on monthly to decadal time scales. These indices can be found on the website of the NOAA at <https://psl.noaa.gov/data/climateindices/list/>, last time accessed on March 2021. The specific selection is made to clarify the dependencies between the Tropical and North Pacific Basins, and the North Atlantic basin, together with their possible influence on Western Europe at midlatitude. For a detailed discussion of several of these indices, please see Deser et al. (2010).

- The Pacific North American (PNA) Pattern is a dominant mode of variability in the extratropical regions over the Pacific. In its positive phase, the atmosphere over the Pacific is characterized by an enhanced East Asian jet stream and an eastward shift of the jet exit region toward the western United States, while in the negative phase a westward displacement of the jet stream toward eastern Asia is experienced. This is associated with much less zonal dynamics, e.g., Wallace and Gutzler (1981).
- The North Atlantic Oscillation (NAO) pattern is also a dominant mode of variability characterized by basin-wide changes of the variability of the jet stream over the North Atlantic, Barnston and Livezey (1987).
- The Arctic Oscillation (AO) is an index based on the projection of the 1000hPa height anomalies on its first EOF pattern poleward of 20° North, Thompson and Wallace (1998).
- The Atlantic Multidecadal Oscillation (AMO) is the standardized index of the projection of the Sea Surface Temperature in the Pacific (detrended) poleward 20N on the dominant Empirical Orthogonal Function, e.g., Enfield et al. (2001). Note that detrending the data to remove the long-term climate change signal in the sea surface temperature could have some impact on the amplitude and the phase of the AMO signal as discussed in Mann et al. (2014).
- The Pacific Decadal Oscillation (PDO) is, as the AMO, the standardized index of the projection of the Sea Surface Temperature in the Pacific (detrended) poleward 20N on the dominant Empirical Orthogonal Function, e.g., Deser et al. (2010).

- The Tropical North Atlantic (TNA) index is the dominant-EOF-based reconstructed time series of the Sea Surface Temperature (detrended) anomalies of the Tropical North Atlantic region 5.5N–23.5N, 57.5W–15W, Enfield et al. (1999).
- The well-known Niño 3.4 index corresponds to the standardized anomaly of Sea Surface Temperature in the Tropical region 5S–5N, 170W–120W. This will be referred to as El-Niño in the sequel or Nino in the figures.
- Three monthly time series of temperature, precipitation and insolation (hours per months) recorded at the reference station Uccle-Ukkel in Belgium. These three monthly time series are available in a supplementary file.

All these monthly indices and time series cover the period from January 1950 to December 2020. The time series for the El-Niño 3.4 and the temperature T2m in Uccle-Ukkel are both linearly detrended to get a stationary time series. The analysis is done using monthly anomalies, after removing the monthly means.

3. THE METHOD

3.1 THE LIANG-KLEEMAN INFORMATION TRANSFER

The last decades have seen the development of techniques to disentangle the dependencies between different observables, going beyond the classical correlation analysis, e.g. Liang (2014a;b; 2016; 2021). These techniques are belonging to the field of causal inference. Traditionally causal inference has been formulated as a statistical testing problem ever since the seminal work by Granger (1969). Recently it is found that causality is actually a real physical notion that can be rigorously derived from first principles (Liang, 2016) in terms of information transfer, or information flow as it is referred to in the literature. Though with a rich history of research for more than 40 years, information transfer has just been rigorously formulated, initially motivated by the predictability study and data assimilation in atmosphere-ocean science (Liang and Kleeman 2005). Since then it has been validated with many benchmark dynamical systems such as baker transformation, Hénon map, Rössler system, etc. (cf. Liang 2016), and has been applied with success to problems in different disciplines; refer to Liang (2021), section 2, for a gentle stroll of the material. The following is just a brief introduction of the concepts and formulae that pertain to this study.

Consider a dynamical system

$$d\mathbf{X} = \mathbf{F}(t; \mathbf{X})dt + \mathbf{B}(t; \mathbf{X})d\mathbf{W}, \quad (1)$$

where $\mathbf{X} = (X_1, X_2, \dots, X_\nu)^T$ is a ν -dimensional vector of state variables, \mathbf{F} a vector of functions, $\mathbf{B} = (b_{ij})$ a ν -by- m matrix of stochastic perturbation amplitudes, and \mathbf{W} an m -vector of standard Wiener processes ($\dot{\mathbf{W}}$ stands for

a vector of white noises). As conventional, a random variable is denoted with an upper-case symbol, and the corresponding deterministic variable is denoted with its lower-case counterpart.

Under a weak assumption that \mathbf{F} and \mathbf{B} are differentiable vector functions, Liang (2016) established that the amount of Shannon entropy, also known as self-information (e.g., Cover and Thomas, 1991), transferred from X_2 to X_1 per unit time, is:

$$T_{2 \rightarrow 1} = - E \left[\frac{1}{\rho_1} \int_{\mathbb{R}^{\nu-2}} \frac{\partial(F_1 \rho_x)}{\partial x_1} dx_3 \dots dx_\nu \right] + \frac{1}{2} E \left[\frac{1}{\rho_1} \int_{\mathbb{R}^{\nu-2}} \frac{\partial^2(g_{11} \rho_x)}{\partial x_1^2} dx_3 \dots dx_\nu \right], \quad (2)$$

where E stands for mathematical expectation, $\rho_1 = \rho_1(x_1)$ is the marginal probability density function (pdf) of X_1 , $\rho_x = \int_{\mathbb{R}} \rho dx_2$, and $g_{11} = \sum_{j=1}^m b_{1j} b_{1j}$. $T_{2 \rightarrow 1}$ is the information transfer from X_2 to X_1 (in nats per unit time); also it is often referred to as information flow. In literature information transfer and information flow are used interchangeably. Ideally if $T_{2 \rightarrow 1} = 0$, then X_2 is not causal to X_1 ; otherwise it is causal (for either positive or negative values). But in practice significance test is needed.

It has been established that $T_{2 \rightarrow 1}$ is generally not equal to $T_{1 \rightarrow 2}$, this is the asymmetry of causality between two variables, in contrast to the symmetric form of correlation. Correlation/association will be established between two variables, say X_1 and X_2 , due to the following five reasons:

- (1) X_1 causes X_2 but X_2 is not causal to X_1 ;
- (2) X_2 causes X_1 but not the other way around;
- (3) X_1 and X_2 are mutually causal;
- (4) X_1 and X_2 are not directly linked but both are caused by a common driver, say X_3 ;
- (5) X_1 (X_2) causes X_2 (X_1) via n other intermediate variables.

These cases, which are difficult to disentangle in statistics, can be easily distinguished, thanks to a property of information flow/transfer, which asserts that, if the evolution of X_1 is independent of X_2 , then $T_{2 \rightarrow 1} = 0$. This ‘‘principle of nil causality’’ is a quantitative fact that all causality analyses try to verify in applications, while here it is a proven theorem. More often than not, for cases 1–3, it is easy to conclude with a mutually causal relation; for cases 4 and 5, spurious causal relation may result. But in the framework of information flow/transfer, these are not problems, at least from a theoretical point of view. Particularly, for case 5, there is no direct causal relation between X_1 and X_2 , but there does exist causality between a series with the delayed series of another (delayed by n step).

Generally $T_{2 \rightarrow 1}$ depends on (x_3, \dots, x_ν) as well as (x_1, x_2) , and, as shown above, the order of the variables. But it has been established that (Liang, 2018) $T_{2 \rightarrow 1}$ in (2) is

invariant upon arbitrary nonlinear transformation of (x_3, x_4, \dots, x_ν) , indicating that information flow is an intrinsic physical property.

With an assumption of linear systems and the noises are independent, the formula (2) can be greatly simplified, and, moreover, easily estimated based on observational data (Liang 2014b; 2021). Suppose we have ν time series, $X_i, i = 1, \dots, \nu$, and these series are equi-spaced, all having N data points $X_i(n), n = 1, 2, \dots, N$. Generate a new series \dot{X}_i such that

$$\dot{X}_i(n) = \frac{X_i(n+1) - X_i(n)}{\Delta t}$$

where Δt is the time stepsize (not essential; only affect the units). Let C_{ij} be the sample covariance between X_i and X_j , and $C_{i,dj}$ the sample covariance between X_i and \dot{X}_j . It has been shown that the maximum likelihood estimator (MLE) of the information transfer from X_2 to X_1 is

$$\hat{T}_{2 \rightarrow 1} = \frac{1}{\det \mathbf{C}} \cdot \sum_{j=1}^{\nu} \Delta_{2j} C_{j,d1} \cdot \frac{C_{12}}{C_{11}}, \quad (3)$$

where Δ_{ij} are the cofactors of the covariance matrix $\mathbf{C} = (C_{ij})$, and $\det \mathbf{C}$ is the determinant of \mathbf{C} . Same can be done to derive the MLE of $T_{1 \rightarrow 2}$, $\hat{T}_{1 \rightarrow 2}$. But the easiest way is simply to swap the indices in (3).

When $\nu = 2$, the above equation reduces to

$$\hat{T}_{2 \rightarrow 1} = \frac{C_{11}C_{12}C_{2,d1} - C_{12}^2C_{1,d1}}{C_{11}^2C_{22} - C_{11}C_{12}^2} \quad (4)$$

This is the MLE of the bivariate information flow/transfer as obtained in Liang (2014b) and frequently used in applications.

As the adage goes, causation implies correlation, but correlation does not imply causation. In (3), when two variables, here X_1 and X_2 , are not correlated, $C_{12} = 0$, then $T_{2 \rightarrow 1} = T_{1 \rightarrow 2} = 0$. But it does not hold conversely. The formulas for $T_{2 \rightarrow 1}$ and $T_{1 \rightarrow 2}$ hence provides a transparent mathematical expression for the interpretation of the adage.

It should be noted that (3) is just the MLE of (2). Beside, in real applications, whether a quantity vanishes should be asked statistically whether it is significantly different from zero. So significance test is needed for the calculated $T_{2 \rightarrow 1}$ and $T_{1 \rightarrow 2}$. A simple way has been proposed with the aid of Fisher information matrix; see Liang (2021). More sophisticated method is yet to be implemented, however. Here we will use a bootstrap method with replacement, as in Vannitsem et al. (2019).

Note that the results that will be presented in the following are normalized in such a way that all influences of one specific observable are put on the same ground. It will give a percentage of influence of the 9 other observables on the target one. The normalization factor in the multivariate case is as in Liang (2021):

$$Z_1 = \left| \frac{dH_1^*}{dt} \right| + \sum_{j=2}^{\nu} |T_{j \rightarrow 1}| + \left| \frac{dH_1^{noise}}{dt} \right|$$

where $\left| \frac{dH_1^*}{dt} \right|$ and $\left| \frac{dH_1^{noise}}{dt} \right|$ are the self-contribution and the noise contribution, respectively.

The relative transfer of information from X_2 to X_1 is then given by,

$$\tau_{2 \rightarrow 1} = \frac{T_{2 \rightarrow 1}}{Z_1}$$

This quantity will be displayed for the set of observable presented at section 2, for all the pairs of observables.

3.2 THE AVERAGING METHOD

A key objective of climate modelling is to describe the dynamics of the moments of the short-scale atmospheric variability (mean, variance...) on time scales from seasons to centuries. The current approach of that problem is to numerically integrate a comprehensive Earth system model including all the details of the dynamics of all its components and to compute moments of the short scale variables. This highly computer time demanding approach is however not the only one. A systematic derivation of the dynamical equations for these moments is an alternative approach that has been started some years ago, e.g. Nicolis and Nicolis (1995; 1998); Vannitsem and Nicolis (1998); Essex (2011). In Essex (2011), the difficulties of developing such equations are discussed, which is probably one of the most challenging mathematical problems of our time. In the approaches developed in that direction so far, one possible averaging approach is the running mean defined as

$$\bar{q}(t) = \frac{1}{S} \int_{-S/2}^{S/2} d\tau q(t + \tau) \quad (5)$$

where q is one variable of the system. This type of averaging acts as a low-pass filter, Nicolis and Nicolis (1995), which has been used in many different context to investigate the climate dynamics, e.g. Saltzman (1983), the predictability in the extended range, e.g. Roads (1987); Vannitsem and Nicolis (1998), or more advanced properties of the attractor of the climate system, e.g. Faranda et al. (2019).

This type of averaging is adopted here, as it allows for filtering out high frequencies, while keeping a number of data points of the same order as the original time series.

The impact of the averaging method is to filter small-scale variability, and to select slower time scales. In the computation of the rate of information flow, the impact is twofold: (i) the fast variability (zero-mean noise) around the sliding average are removed, and (ii) while taking the difference of sliding averages, the tendencies become discrete time derivatives on a time scale $S = L\Delta t$.

4. RESULTS

The analysis is split into 3 different regions. First, the focus is placed on the two-way dependencies of the indices over the Tropical and North Pacific. Second, the analysis

will focus on the North Atlantic region and the Arctic, and finally, the dependencies of the local observables over Belgium are investigated.

4.1. PACIFIC DEPENDENCE PATTERNS

Figure 1 displays the rate of transfer of information between El-Niño 3.4 and all the other observables listed in Section 2. In each panel, two curves are displayed as a function of the sliding window used for averaging, a curve for the rate of information transfer from one observable to El-Niño 3.4 (squares, red curve) and a curve with the rate of information transfer from El-Niño to the same observable. In that way the asymmetry of transfer of information can be evaluated. The quantity is normalized as discussed in Section 3.1. A bootstrap method with replacement is used to infer the uncertainty of these quantities. When the zero line is crossing the error bar at the 95% dependence is assumed.

This approach is challenged in Appendix 8 by building a surrogate dataset based on the original data themselves, which revealed that the approach proposed is appropriate. It is however important to mention that the multiplication of tests opens the possibility of an increase number of false positive. So when the zero line is close to the margins of the bootstrap sampling, the alleged dependencies should be taken with caution. This is kept in mind when discussing the results.

One key feature appearing in this figure is the strong link between the PNA and El-Niño on time scales from, say, a few months until 4 years (panel (d)). PNA contributes for more than 30% indicating that PNA tends to constrain the variability of El-Niño. On the other hand, El-Niño is also influencing PNA, but now with a positive value, suggesting that El-Niño tends to increase the variability of PNA. A similar influence of El-Niño on PDO is found (panel e), but now PDO does not influence El-Niño. This type of dependencies over the Pacific are already well documented, see for instance Lin and Derome (2004); Liu and Alexander (2007); Newman et al. (2016), but this analysis provides a clear indication of the presence of a dynamical dependence together with the type of constraint imposed by one variable on the other. Interestingly the key role played by El-Niño on PDO at all scales put forward by Newman et al. (2003; 2016) and the role of the atmospheric variability over the North Pacific on El-Niño discussed in Ding et al. (2017) are indeed confirmed by the analysis.

Another important dependence on a shorter time scale is found between TNA and El-Niño (panel g). TNA influences El-Niño on time scales of a few months, constraining its variability. While El-Niño is influencing TNA for a larger range of sliding windows up to a bit more than 2 years, tending to increase the variability of TNA. This control on cross-basins is clearly occurring on seasonal to interannual time scales.

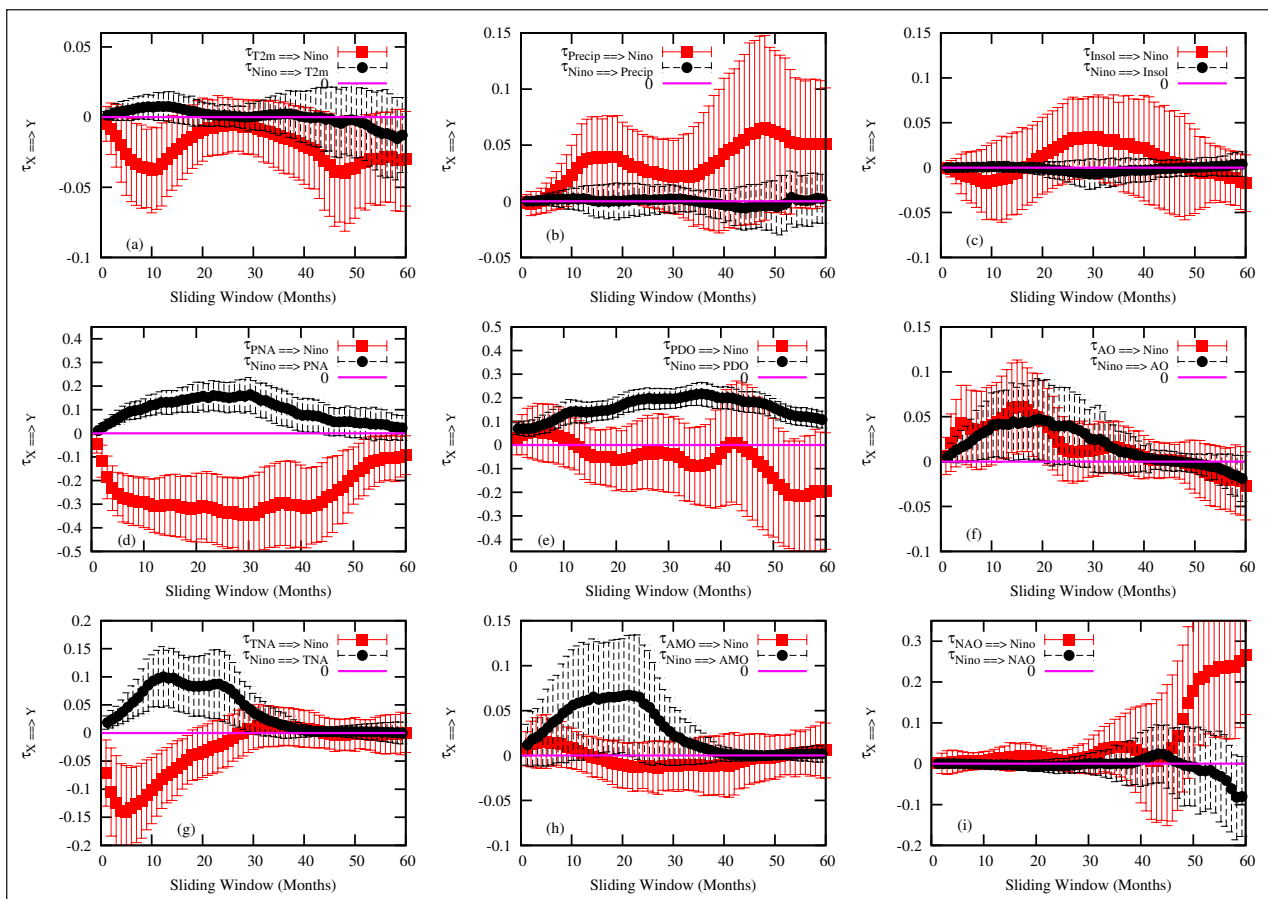


Figure 1 The rate of information transfer as a function of the averaging sliding window. All interactions with El-Niño 3.4.

In panel (i) the dependencies between NAO and El-Niño are depicted. It is interesting to note that there is no dependence detected by the Liang-Kleeman method from El-Niño to NAO, but contrarily an important dependence is found from NAO to El-Niño for large sliding windows, suggesting an influence of NAO on the Low-frequency variability of El-Niño at these slow time scales. To our knowledge this feature has not been reported yet and seems not to be supported by other analysis of dependencies based on the Granger causality approach, see Mokhov and Smirnov (2006). This question is worth investigating further in more details with other approaches and in a similar analysis setting in the future.

For the other observables, dependencies are not detected, except marginally between the AO and El-Niño (panel f), from El-Niño on AMO (panel h), and from T2m on El-Niño (panel a). The latter is rather surprising, but it would suggest that the extratropical dynamics over the continental zones also display an influence on the Tropical pacific dynamics. This will be discussed further in Section 4.3.

A second important pattern is the Pacific North America pattern, known to play an important role in the dynamics in the extratropics, see e.g. Liu and Alexander (2007). *Figure 2* shows the rate of information transfer from and to PNA, based on the ensemble of variables as for El-Niño. Panel (f) has already been discussed

when discussing the results of *Figure 1*, but kept here for consistency with the other figures.

A first very interesting feature appearing in panels (a) and (b) is the dependence of the T2m and Precipitation over Belgium to PNA for long sliding windows filtering out high frequencies of the observables. Anticipating the results discussed in Section 4.3, an influence on the LFV over western Europe is associated with PNA, constraining the variability of temperature, but increasing the variability of precipitation.

Another interesting feature is the influence of PNA on PDO, illustrated in panel (e). The black curve shows significant positive values for windows of a few months and significant negative values around 3 years. The high frequency variability of the NAO induces an increase of variability of PDO, but for long averages, the NAO tends to reduce the variability of the PDO, although quite weakly in view of its marginality to 0. The inversion of sign of the dependencies is an interesting feature suggesting that observables can play different roles at different time scales. Such a specific property is worth addressing in the context of simple climate models in order to figure out what are the properties of the models which are driving this type of transition.

Finally, among the other panels, a marginal dependence emerges between the TNA and PNA for large sliding windows. This specific teleconnection is probably

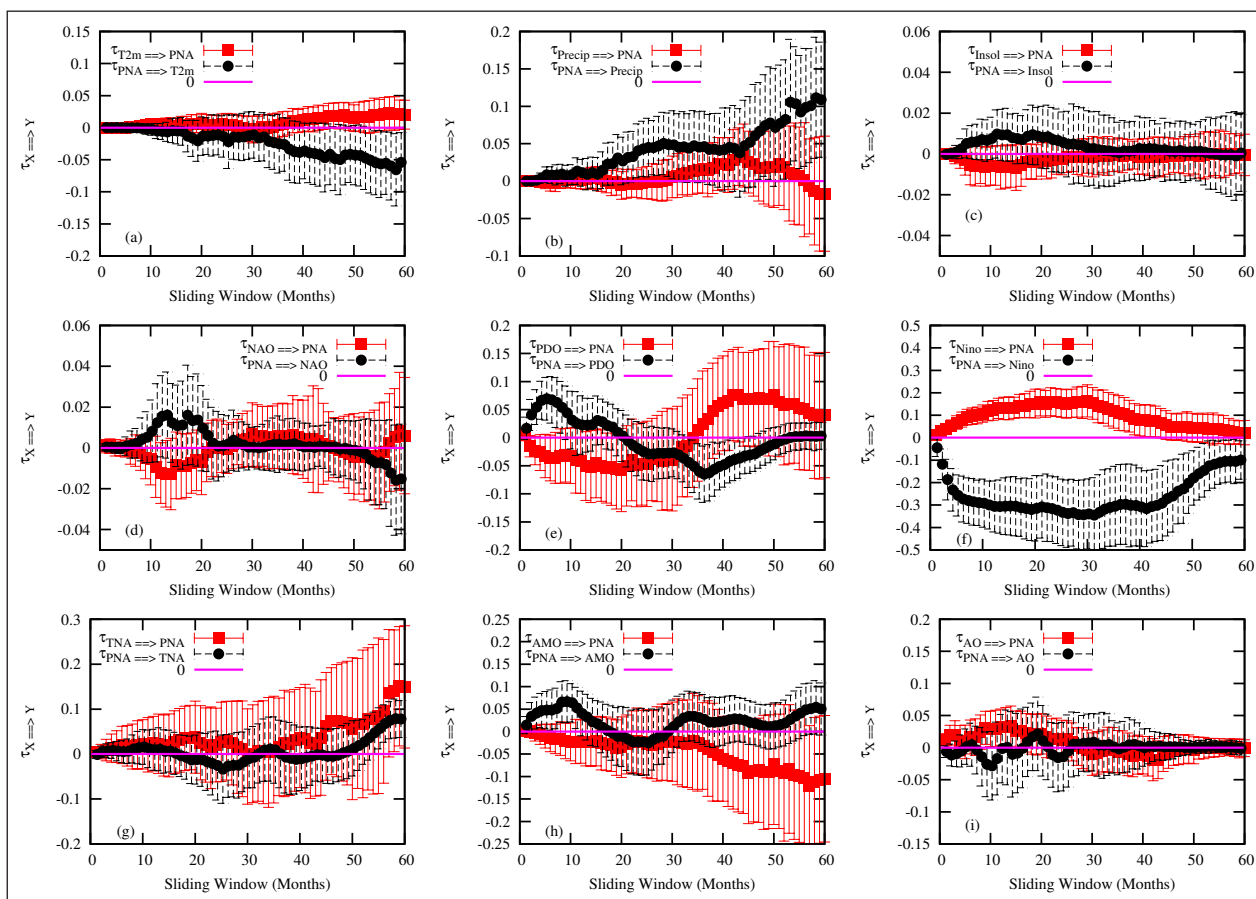


Figure 2 The rate of information transfer as a function of the averaging sliding window. All interactions with PNA.

harder to understand than the others, but we should keep in mind that not all possible observables were selected, which could induce some detection associated with other pathways.

Concerning the influence of PDO, the only pathways found are toward TNA and AMO on long time scales, See Figure A1 in the Appendix. This feature suggests a link between the variability of the different ocean basins. These specific dependencies are still not clear for us at this stage, but the absence of influence of PDO on the majority of the observables tends to confirm the view that PDO is the byproduct of the influence of many different processes as suggested in Newman et al. (2016).

4.2. NORTH ATLANTIC AND ARCTIC DEPENDENCE PATTERNS

Let us now turn to the Arctic-North Atlantic region. In **Figure 3**, the influences from and to AO are displayed. A first remark is to see that the only observable influencing AO is the NAO for very large sliding windows (panel i). The amplitude of this influence is very large and positive. This result suggests that NAO is increasing the low-frequency variability of the AO. On the other hand, the AO is influencing the NAO for shorter sliding windows of the order of the year. A two-way dynamical control is found for these two patterns but on different frequencies of the variability.

Another interesting feature is the influence of AO on the different observables over Belgium for windows at intra-annual time scales (panels a, b and c), suggesting a role of the AO for intra-annual evolution of the climate over Belgium. This role does not seem extremely strong, but is worth investigating further in the future when investigating the possibility for seasonal forecasts over this region.

A slight influence of the AO on PNA, PDO, El-Niño (already reported), and TNA is also emerging at the 95% from a few months to a couple of years.

The analysis of the role of the AO is interesting as it suggests that this pattern is a key driver of the dynamics at different place of the world, and in particular over Western Europe, of the variability of seasonal to interannual time scales.

Let us now turn to the NAO (**Figure 4**). Surprisingly, the NAO does not show any influence on the variability over Belgium (panels a, b and c). It however shows influences on the PDO, El-Niño (already reported), TNA and AO on large sliding windows, reflecting its role on controlling the variability at long time scales. This makes of NAO a key actor of the long term dynamics of the climate system as El-Niño is.

There is also a strong influence of the NAO on AMO on seasonal to interannual windows (panel h). It is however interesting to note that there is no substantial influence of the AMO on NAO at the time scales we are interested in here.

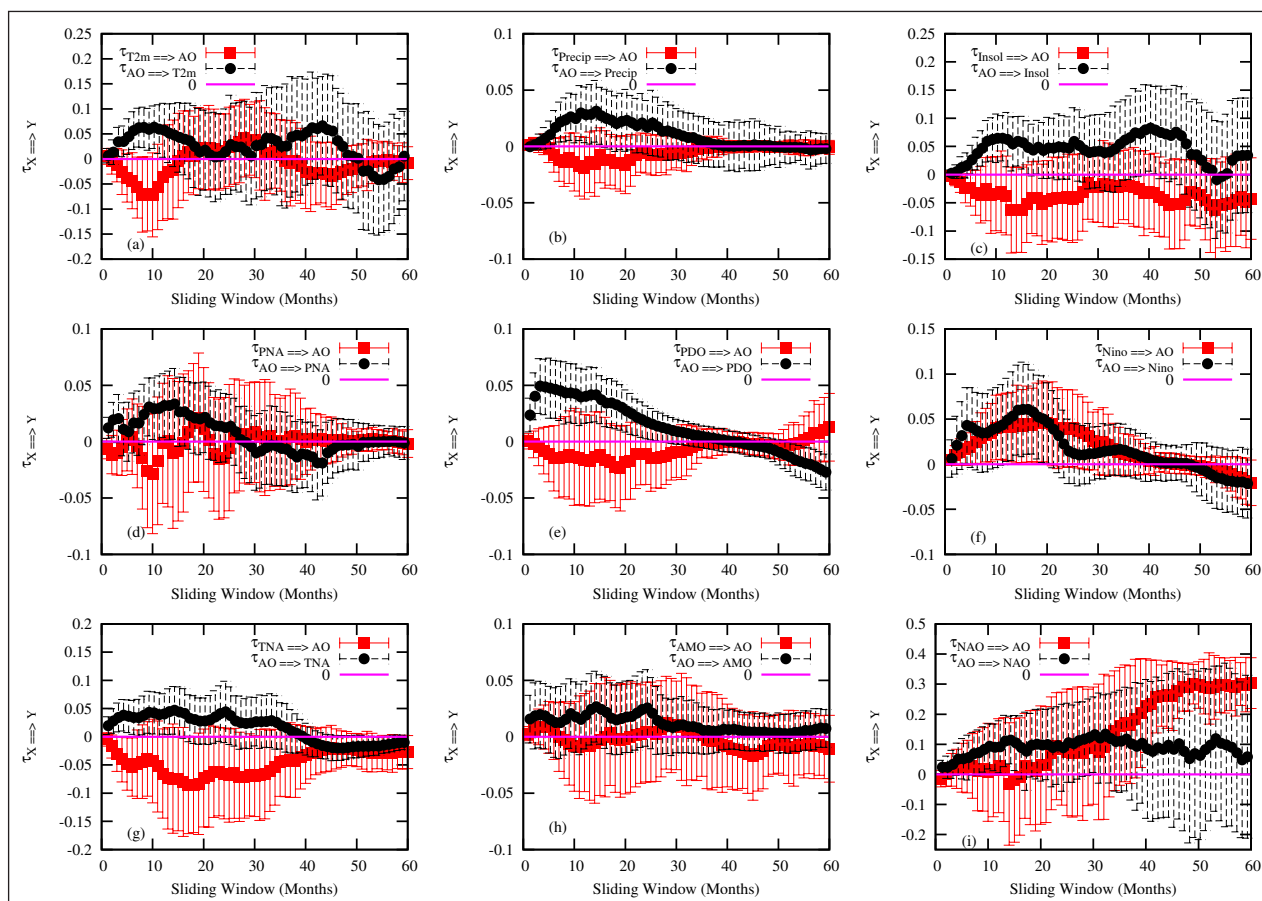


Figure 3 The rate of information transfer as a function of the averaging sliding window. All interactions with AO.

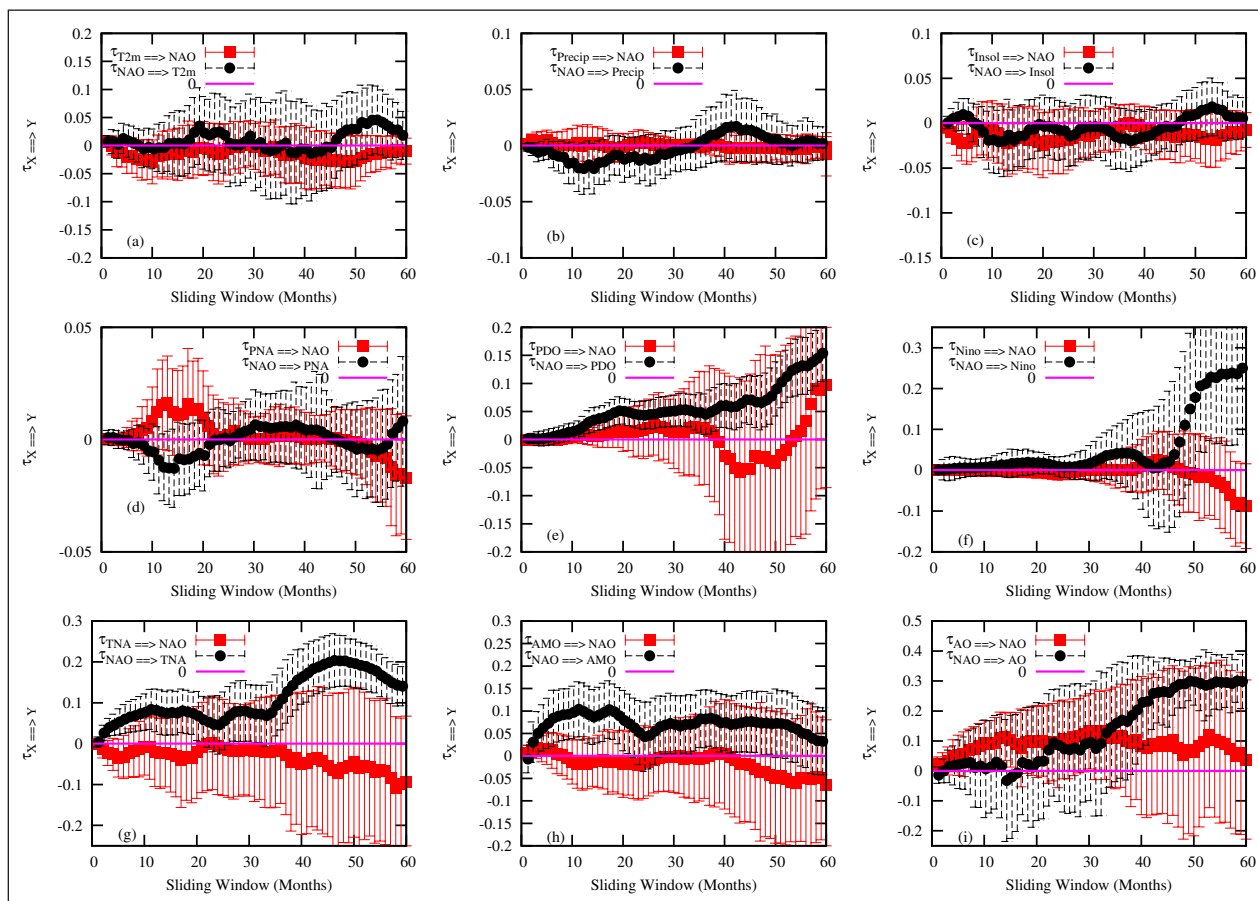


Figure 4 The rate of information transfer as a function of the averaging sliding window. All interactions with NAO.

These results should also help in clarifying the respective role of the AO and NAO in the dynamics of the climate system, as discussed in Ambaum et al. (2001). The AO is driving the variability on different time scales than the NAO, the former being active at short time scales (seasonal to interannual), while NAO on long time scales (from 2–3 years to 5). So both are important, and there is no reason to think that one of them has a more important role to play than the other.

The influence on AMO and TNA are also displayed for completeness in Figs. A2 and A3, respectively. The dominant influence is the two-way interaction between AMO and TNA, which can be explained by their proximity and the presence of ocean tunnels in that region, see Liu and Alexander (2007). The other dependencies with TNA and AMO are explained when discussing the results of the other targeted observables.

4.3. REGIONAL DEPENDENCE PATTERNS OVER BELGIUM

Let us now investigate the dependencies of the observables recorded over Belgium. **Figure 5** displays the dependencies between temperature at 2 meters with the other observables. A first interesting result is the absence of dependencies with the other observables measured locally, precipitation and insolation. These seem to be related to different dynamical processes, even if we could expect some

climatic relationship like the Clausius-Clapeyron relationship linking the water vapor content to the temperature (and hence the precipitation amounts). This type of feature does not appear in the current data analysis.

The only observables that significantly influence the temperature at 2 meters are the AO pattern on short time scales and the PNA pattern on long time scales. These interesting features suggest a possible forecasting system for temperature over Belgium based on these two patterns. This will be explored in the future.

Another interesting result is the (marginal) dependence of PDO and PNA on temperature over Belgium at long time scales. This feature looks quite counter-intuitive. A conjecture is that this link is associated to the long term dependence of PDO and PNA on large-scale Eurasian (or circumglobal) climate dynamics. The positive dependence tends to increase the variability of these patterns.

Finally, there is a marginal influence of temperature on AMO, TNA and El-Niño on time scales from a few months to a few years. Here the negative values suggest a control of the variability by the temperature over Western Europe. Again this feature illustrates the probable influence present from the Eurasian extratropical continent to the tropical region.

For the precipitation displayed in **Figure 6**, the dependence on the large scale modes are the same as for

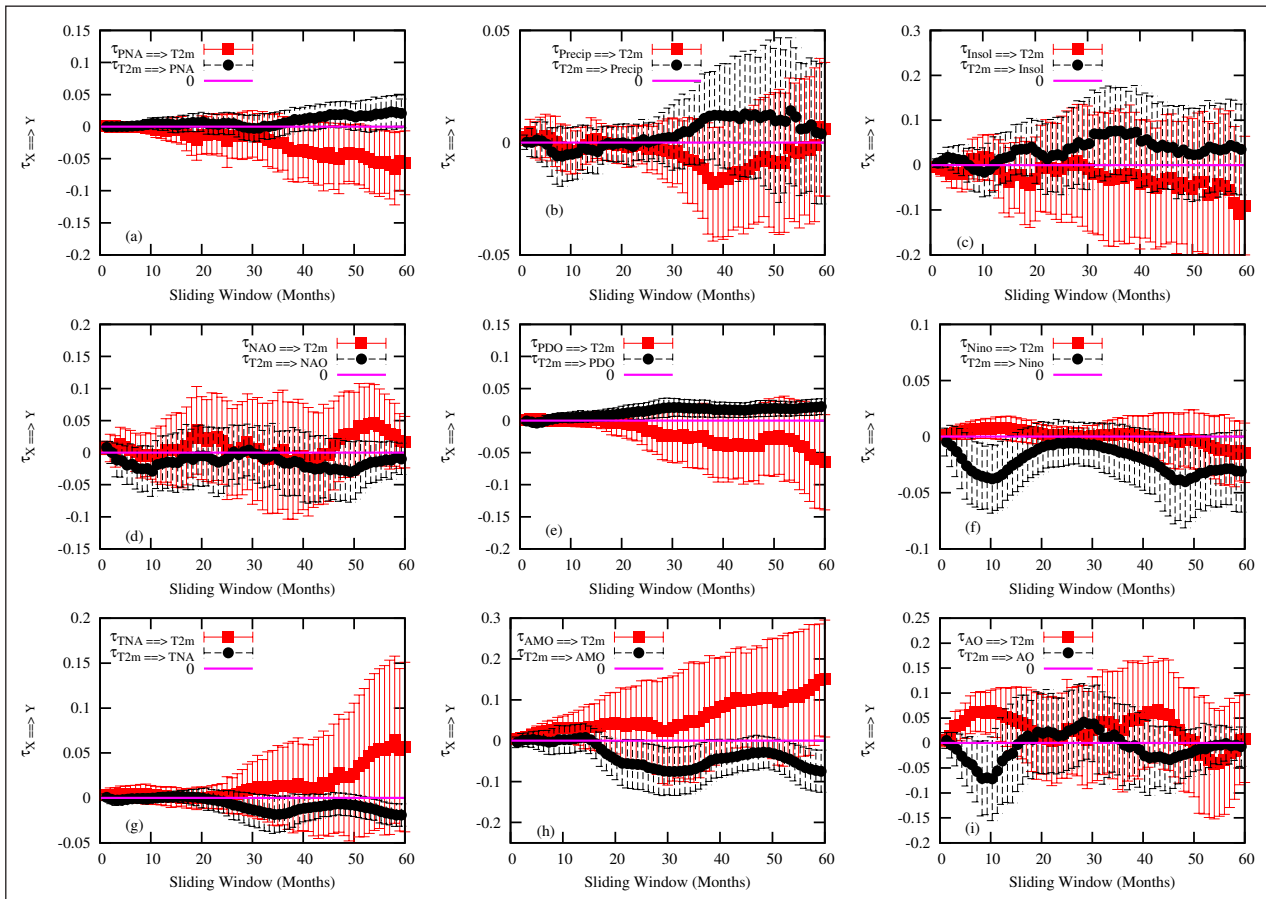


Figure 5 The rate of information transfer as a function of the averaging sliding window. All interactions with T2m.

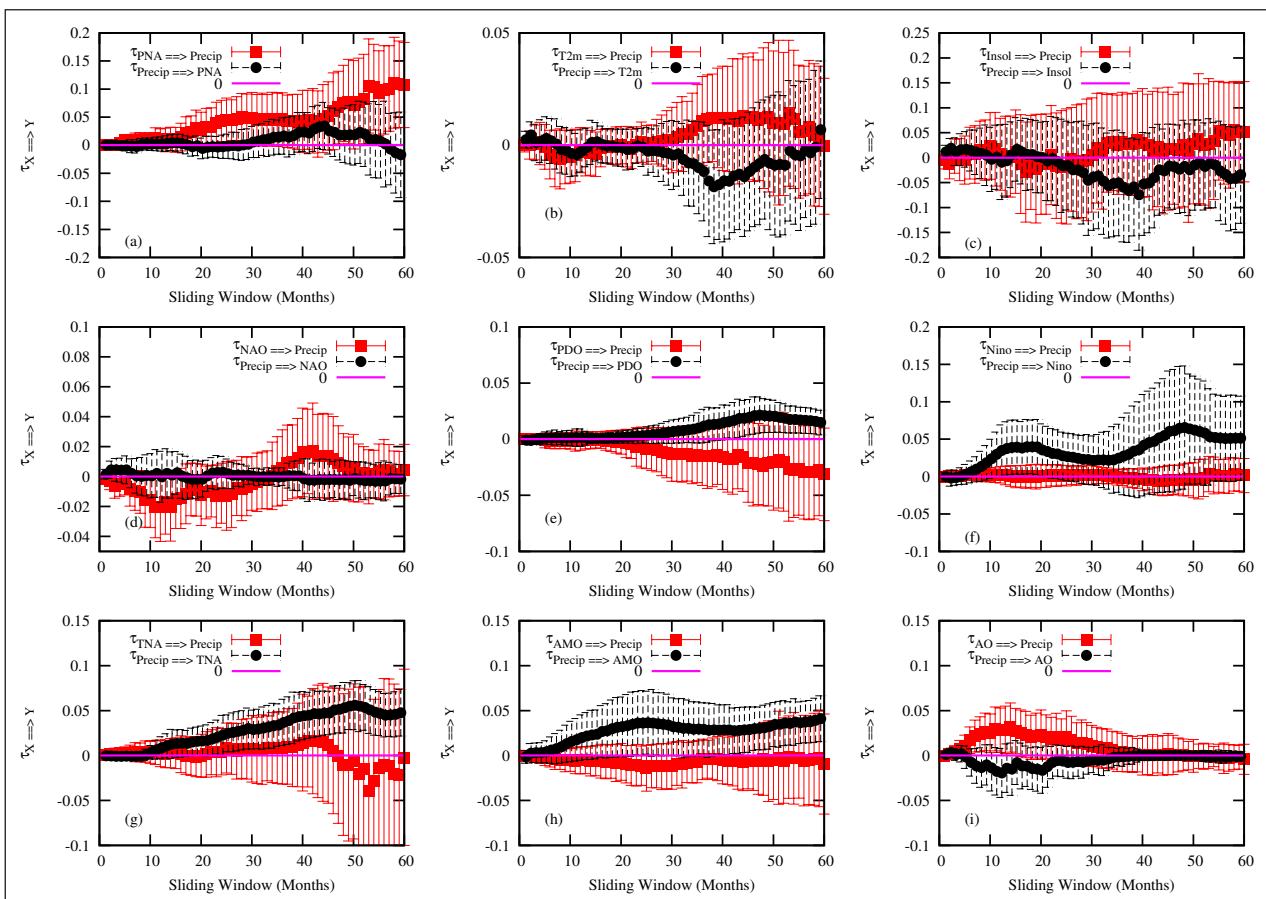


Figure 6 The rate of information transfer as a function of the averaging sliding window. All interactions with Precipitation.

temperature: The AO is influencing the variability of precipitation on short time scales, while on long time scales, this is the PNA influencing precipitation. The fact that both series, which are not showing dependencies between each other, are showing the same dependencies to PNA and AO provide a coherent signal of the dynamical influence of these large-scale atmospheric patterns on our region.

There is also a very interesting signal on the dependence of the PDO, AMO and TNA on precipitation for long time scales. As for temperature, this remote influence from a local variable should reflect a midlatitude influence of circumglobal atmospheric processes on key ocean patterns.

For the insolation (*Figure 7*), the only detected influence is from the AO on short time scale variability. On the other hand, an influence of the insolation is found for the PDO, AMO and TNA. Again the influence of this local variable should reflect the influence of circumglobal atmospheric variability on these patterns.

This particular feature of the local variables is intriguing and calls for additional investigations. The fact that the NAO does not influence the local variables suggests that the NAO and the processes associated with the remote influence of the local variables are not dependent on each other. The long term influence of NAO on AMO, PDO and TNA is probably not the origin of this dependence, unless more complicated nonlinear interactions are

taking place. Is this related to the continental-ocean contrast or to other chains of processes? This is still an open question that cannot be answered without using additional climate indicators.

5. SUMMARY AND CONCLUSIONS

5.1. SUMMARY OF THE DEPENDENCIES

In the present work, a detailed analysis of the dependencies between a set of key climate indices (El-Niño 3.4, PDO, AMO, TNA, PNA, AO, NAO) and three local time series reflecting the local dynamics at monthly time scale over Belgium. The three latter time series have been chosen to clarify the role of large scale climate indices in a region of Western Europe over which long term forecasting are complicated (Cassou et al., 2018; Pegion et al., 2019; Merryfield et al., 2020). The overall results indicate the complex nature of the interactions between the different observables whose dependencies are acting on different time scales.

The dependencies found in the present work can be split into three categories. First the dependencies that are emerging at all time scales explored from a month to 5 years. These involve El-Niño, PNA and PDO in the North and Tropical Pacific and NAO and AMO in the North Atlantic (yellow arrows in *Figure 8*). In this context, PDO and AMO seem to be predominantly driven by El-Niño, PNA and NAO.

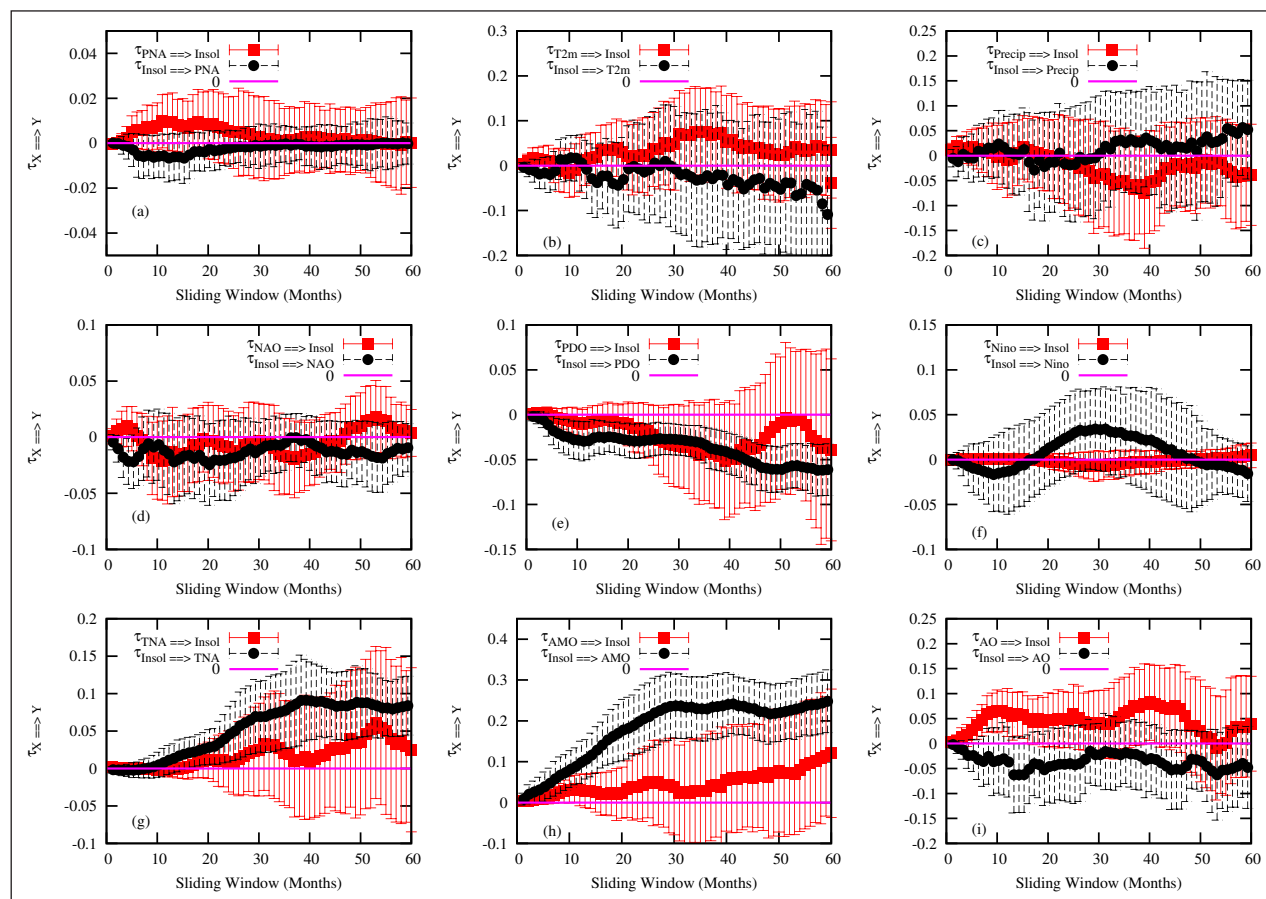


Figure 7 The rate of information transfer as a function of the averaging sliding window. All interactions with Insolation.

The link from NAO to AMO and AMO to PDO, reported in Nigam et al. (2020) is indeed confirmed by our current analysis, although they found cross-correlation links on time lags much larger than the time scales investigated here.

Second the dependencies on the variability at short time scales also displayed in **Figure 8** (blue arrows). There are clearly dependencies within the ocean like for instance between AMO and TNA, probably related to the ocean tunnels, see, e.g., Liu and Alexander (2007). But more interestingly there is a strong influence of AO on many other observables. This influence occurs for sliding windows from a few months to a coupled of years,

capturing seasonal to interannual variability. As such, AO can be considered as playing a key role in the network of dependencies in the climate system.

Finally there are dependencies emerging on long time scales, illustrated in **Figure 9**. In this case, the NAO plays a key role in the dynamics of the Climate system, influencing AO, PDO, TNA, El-Niño. This further indicates that both NAO and AO are key indices of the low-frequency variability of the Climate system but at different time scales. The influence of PDO (negative sign) on NAO reported in Nigam et al. (2020) is not confirmed by our analysis. Rather the opposite influence is found on time scales of the order of a few years.

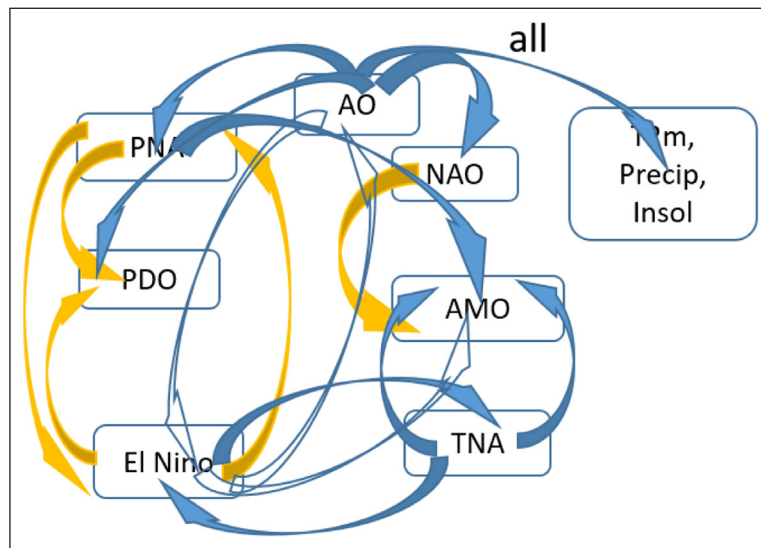


Figure 8 Dependencies between the different observables at short (blue arrows) and all time scales (yellow arrows). The open blue arrows indicate weak dependencies as compared to the other ones. The label “all” indicates that all local variables are influenced by AO.

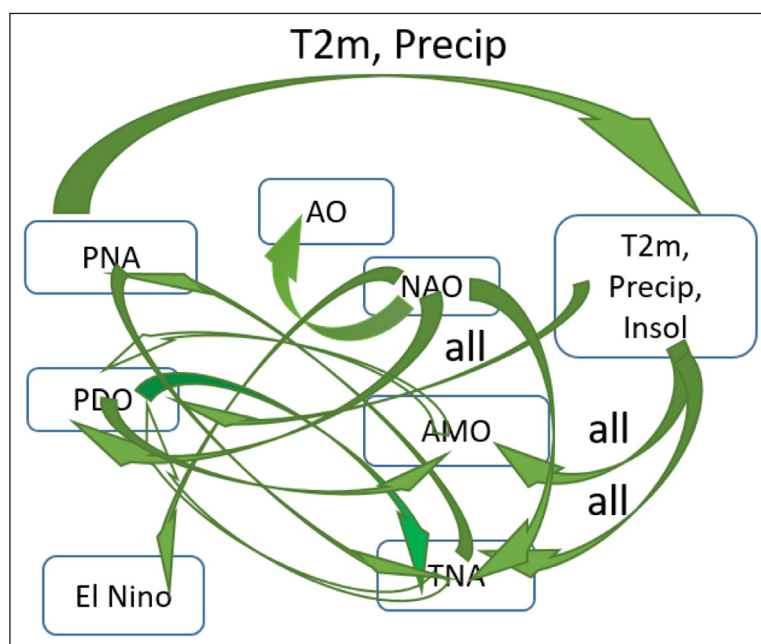


Figure 9 Dependencies between the different observables at long time scales (green arrows). The open green arrows indicate weak dependencies as compared to the other ones. The label “all” indicates that all local observables are influencing the target observable. T2m and Precip refer to temperature at 2 meters and precipitation, respectively.

On the long term, the PNA pattern plays a role in the dynamics of the observables over Belgium. This feature is obviously interesting as it provides potential lines of research to setup forecasting systems at monthly, seasonal and decadal time scales over Belgium. This aspect will be pursued in the future. On the other hand, the observables recorded over Belgium display influences on the AMO, TNA, PDO, and El-Niño. This surprising result suggests that there is an influence of the continental extratropical regions over ocean basins on long time scales. Further analyses are needed using observables at continental scale. A conjecture on these dependencies is that these observables are embedded in the circumglobal circulation teleconnection pattern (CGT) discovered by Branstator (2002), displaying variability on a wide range of time scales, Ding et al. (2011); Soulard et al. (2021); Yang et al. (2021). The Belgium observables may display on long time scale the influence of the CGT, which in turn influences the Tropical Dynamics. This hypothesis is worth exploring in the future.

Other long term influences are also present between PNA and TNA, and between the different ocean components, probably related to the long term dynamics of the world oceans such as the one isolated between PDO and AMO and El-Niño in Johnson et al. (2020).

5.2. LIMITATIONS AND FUTURE APPLICATIONS

The current analysis approach based on the rate of information flow on sliding averages is providing a very interesting way to disentangle the dependencies between indices at various time scales. It confirms some previous dependencies already found, but also indicates that some dependencies are unlikely. It is however clear that we did not use all the possible indices we could think of and limited ourselves to time scales from months to a few years. One possible caveat of our approach is that some dependencies attributed to the observables used are associated with some confounding factors. A possible example is the dependence of El-Niño on the temperature over Belgium. This dependence should probably be associated to a large scale pattern like for instance the circumglobal teleconnection pattern which was not used in the present work. The robustness of the results should therefore be investigated by adding other large scale indices.

This approach should also be used in the context of climate model runs in order to validate the dependencies that are accounted for by the models, and at the same time to confirm the dependencies that have been isolated here on short time series, using long climate model runs. One advantage of using climate models is that ensembles can be used that could further provide temporal information on the changes of dependencies like for instance in the recent applications of Hagan et al. (2019); Docquier et al. (2021), even under transient dynamics.

Finally, The dependencies found for the observables over Belgium could be further explored in order to build a stochastic model that would allow for performing long term forecasts from seasonal to interannual time scales.

APPENDIX A: DEPENDENCIES WITH PDO, TNA AND AMO

The main signals of an influence of PDO on the other observables are found for TNA and AMO as illustrated in [Figure A1](#), while many observables are driving PDO. PDO is mostly controlled by the other key indices of variability.

Concerning the AMO, signals of influence are emerging for the PDO and TNA. A marginal signal is also found from AMO to the T2m over Belgium, see [Figure A2](#).

For the TNA, clear links are emerging between El-Niño and AMO, as already discussed in the main result section. A marginal influence of TNA is also found on PDO and PNA as illustrated in [Figure A3](#).

APPENDIX B: ROBUSTNESS OF THE RESULTS: TEST ON SURROGATES

In order to test the robustness of the results, a usual way to approach the problem is to build surrogates. This usually implies to build a model using assumptions on the statistical and dynamical properties of the series. The time series here have very different statistical and dynamical properties. Building surrogates should therefore be made by defining different models for the different processes at hand. It is clear for instance that for El-Niño, strong asymmetry exists that should be taken into account properly. Still the results based on these surrogates would be highly dependent on the assumptions made for the description of the time series.

An alternative to such an approach is to construct new series from the current series keeping as far as possible the statistical and dynamical properties of these observations. Here we propose to shift in time by a certain amount of months a few series, desynchronizing in that way the dataset. The shift is done in such way that the shifted data beyond the length of the series are now placed at the beginning of the time series. This approach allows for keeping both the nature of the temporal dependencies and the probability distribution of the data. This of course leads to a discontinuity at one place of the shifted series. We here assume that this discontinuity will not play a major role, and we also make sure that the tendency evaluated at this discontinuity point is fixed to 0 in order to avoid big

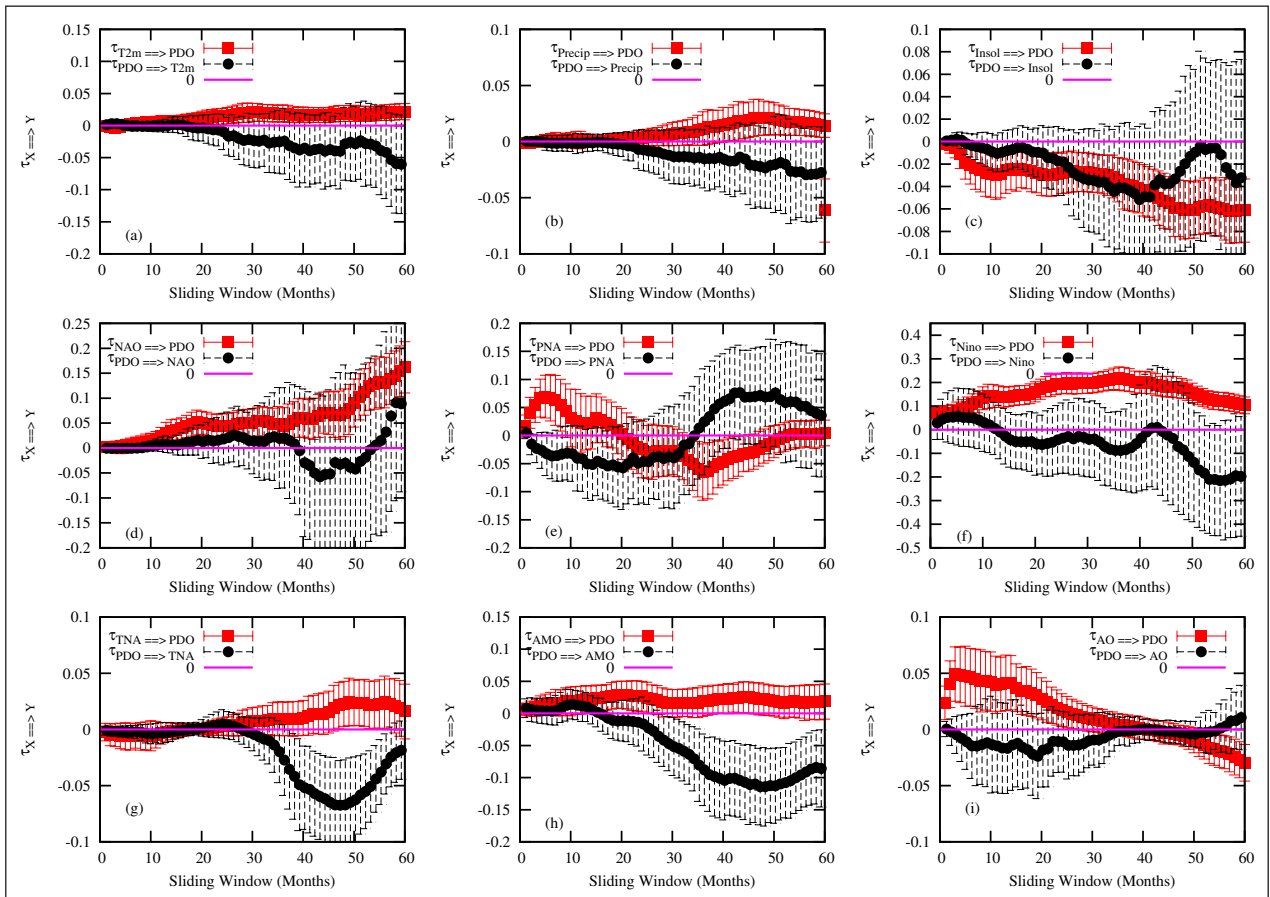


Figure A1 The rate of information transfer as a function of the averaging sliding window. All interactions with PDO.

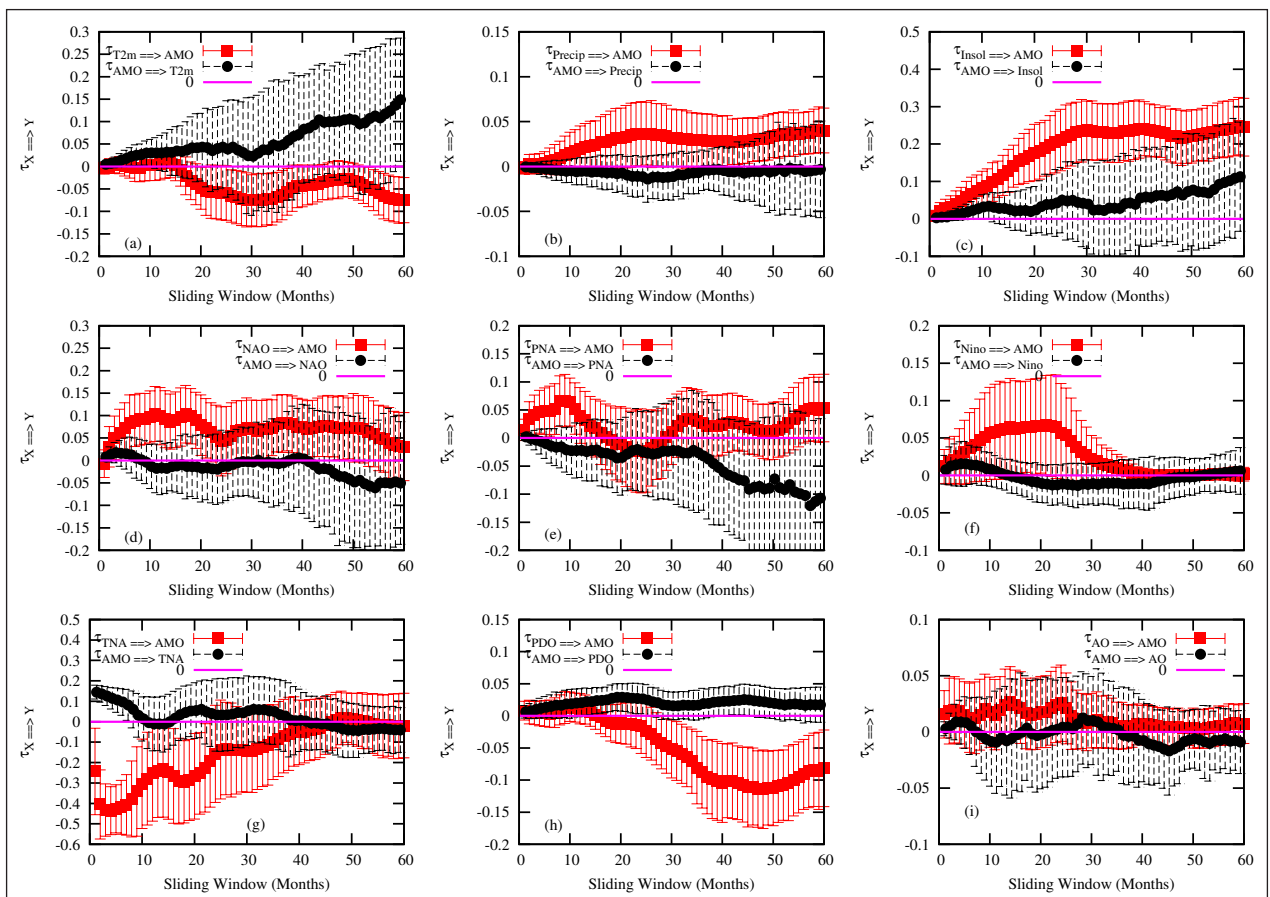


Figure A2 The rate of information transfer as a function of the averaging sliding window. All interactions with AMO.

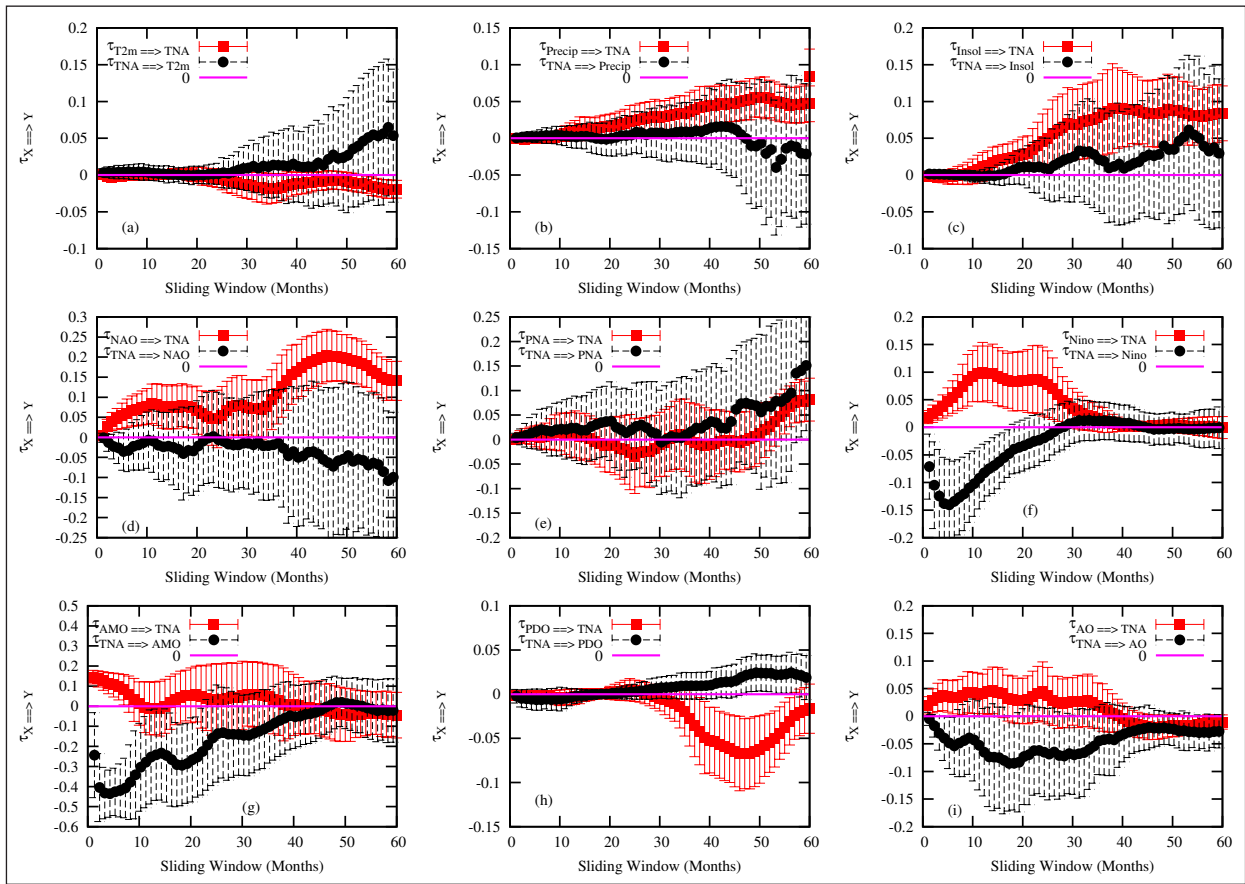


Figure A3 The rate of information transfer as a function of the averaging sliding window. All interactions with TNA.

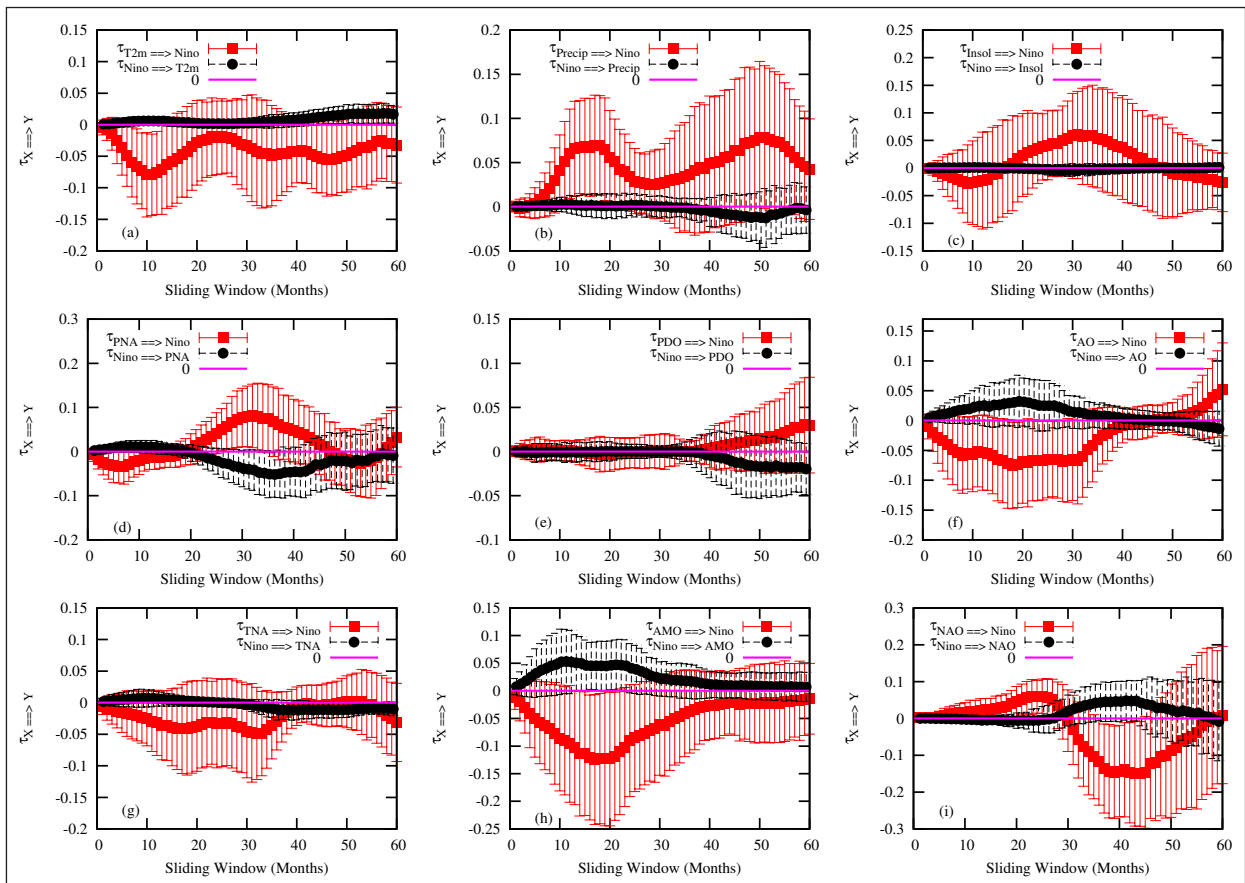


Figure B1 The rate of information transfer as a function of the averaging sliding window. All interactions with El-Niño. Four time series are shifted in time: NAO, PNA, TNA and PDO series by amounts of 200 and 500, 300 and 700 months, respectively.

spurious tendencies. A second assumption is to suppose that there are no large delays in the dependencies. Based on this assumption, we shift several time series by a certain amount of months, larger than the time scales of interest in the present work.

The series that were shifted are the NAO, PNA, TNA and PDO series that were found to show very strong dependencies with the El-Niño series. NAO, PNA, TNA and PDO series are shifted toward positive times by amounts of 200 and 500, 300 and 700 months respectively. This choice (slightly arbitrary) is made in order to well desynchronize the two atmospheric series and the two ocean series, and at the same time to well desynchronize them from the El-Niño series (and avoid any strong delayed dependencies). The other series are not touched upon as they do not show strong dependencies with El-Niño.

The results are displayed in **Figure B1**. All the original dependencies with NAO, PNA, TNA and PDO with El-Niño now disappeared (panels (d), (e), (g) and (i)), indicating that the strong dependencies found originally are associated with links which are synchronous in time. Moreover, the Liang-Kleeman quantities computed for the other time series with the El-Niño one do not change much. We only observe slight modifications of the amplitudes of the mean and of the spread around the mean of the bootstrap evaluations. A change should be expected as the estimations are now made with a different set of 10 time series with a normalization that depends on all dependencies. One particularly interesting feature present in the dependencies between the temperature at 2 meters in Uccle and El-Niño still persists at the 95% level. This supports the robustness of our estimates.

ACKNOWLEDGEMENTS

We would like to thank Michel Journée for providing us the data of the Uccle station. This work was supported by The Belgian Science Policy (Belspo) under Grant B2/20E/P1/ROADMAP.

COMPETING INTERESTS

The authors have no competing interests to declare.

AUTHOR AFFILIATIONS

Stéphane Vannitsem  orcid.org/0000-0002-1734-1042
Royal Meteorological Institute of Belgium, Brussels, Belgium

X. San Liang  orcid.org/0000-0001-8472-3211
Department of Atmospheric and Oceanic Sciences, Fudan University, Shanghai, China

REFERENCES

- Alexander, MA, Blad, I, Newman, M, Lanzante, JR, Lau, N-C and Scott, JD.** 2002. The atmospheric bridge: The influence of ENSO teleconnections on air-sea interaction over the global oceans. *J. Climate*, 15: 2205–2231. DOI: [https://doi.org/10.1175/1520-0442\(2002\)015<2205:TABTI O>2.0.CO;2](https://doi.org/10.1175/1520-0442(2002)015<2205:TABTI O>2.0.CO;2)
- Ambaum, MHP, Hoskins, BJ and Stephenson, DB.** 2001. Arctic oscillation or north Atlantic oscillation? *Journal of Climate*, 14(16): 3495–3507. DOI: [https://doi.org/10.1175/1520-0442\(2001\)014<3495:AONAO>2.0.CO;2](https://doi.org/10.1175/1520-0442(2001)014<3495:AONAO>2.0.CO;2)
- Barnston, AG and Livezey, RE.** 01 Jun. 1987. Classification, seasonality and persistence of low-frequency atmospheric circulation patterns. *Monthly Weather Review*, 115(6): 1083–1126. DOI: [https://doi.org/10.1175/1520-0493\(1987\)115<1083:CSAPOL>2.0.CO;2](https://doi.org/10.1175/1520-0493(1987)115<1083:CSAPOL>2.0.CO;2)
- Branstator, G.** 2002. Circumglobal teleconnections, the jet stream waveguide, and the north Atlantic oscillation. *Journal of Climate*, 15(14): 1893–1910. DOI: [https://doi.org/10.1175/1520-0442\(2002\)015<1893:CTJSW>2.0.CO;2](https://doi.org/10.1175/1520-0442(2002)015<1893:CTJSW>2.0.CO;2)
- Cassou, C, Kushnir, Y, Hawkins, E, Pirani, A, Kucharski, F, Kang, I-S and Caltabiano, N.** 2018. Decadal climate variability and predictability: Challenges and opportunities. *Bulletin of the American Meteorological Society*, 99(3): 479–490. DOI: <https://doi.org/10.1175/BAMS-D-16-0286.1>
- Cover, T and Thomas, J.** 1991. *Elements of Information Theory*. New York, USA: Wiley. DOI: <https://doi.org/10.1002/0471200611>
- Deser, C, Alexander, MA, Xie, S-P and Phillips, AS.** (2010). Sea surface temperature variability: Patterns and mechanisms. *Annual Review of Marine Science*, 2(1): 115–143. DOI: <https://doi.org/10.1146/annurev-marine-120408-151453>
- Di Capua, G, Kretschmer, M, Donner, RV, van den Hurk, B, Vellore, R, Krishnan, R and Coumou, D.** 2020. Tropical and mid-latitude teleconnections interacting with the Indian summer monsoon rainfall: a theory-guided causal effect network approach. *Earth System Dynamics*, 11(1): 17–34. DOI: <https://doi.org/10.5194/esd-11-17-2020>
- Ding, Q, Wang, B, Wallace, JM and Branstator, G.** 2011. Tropical-extratropical teleconnections in boreal summer: Observed interannual variability. *Journal of Climate*, 24(7): 1878–1896. DOI: <https://doi.org/10.1175/2011JCLI3621.1>
- Ding, R, Li, J, Tseng, Y-H, Sun, C and Xie, F.** 2017. Joint impact of north and south Pacific extratropical atmospheric variability on the onset of enso events. *Journal of Geophysical Research: Atmospheres*, 122(1): 279–298. DOI: <https://doi.org/10.1002/2016JD025502>
- Docquier, D, Vannitsem, S, Ragone, F, Wyser, K and Liang, X.** 2021. Causal links between Arctic sea ice and its potential drivers based on the rate of information transfer. *Geophys. Res. Lett.* submitted. DOI: <https://doi.org/10.1002/essoar.10507846.1>

- Enfield, DB, Mestas-Nuez, AM, Mayer, DA and Cid-Serrano, L.** 1999. How ubiquitous is the dipole relationship in tropical Atlantic sea surface temperatures? *Journal of Geophysical Research: Oceans*, 104(C4): 7841–7848. DOI: <https://doi.org/10.1029/1998JC900109>
- Enfield, DB, Mestas-Nuez, AM and Trimble, PJ.** 2001. The Atlantic multidecadal oscillation and its relation to rainfall and river flows in the continental U.S. *Geophysical Research Letters*, 28(10): 2077–2080. DOI: <https://doi.org/10.1029/2000GL012745>
- Essex, C.** 2011. Climate theory versus a theory of climate. *International Journal of Bifurcation and Chaos*, 21(12): 3477–3487. DOI: <https://doi.org/10.1142/S0218127411030672>
- Faranda, D, Messori, G and Vannitsem, S.** 2019. Attractor dimension of time-averaged climate observables: Insights from a low-order ocean-atmosphere model. *Tellus A: Dynamic Meteorology and Oceanography*, 71(1): 1554413. DOI: <https://doi.org/10.1080/16000870.2018.1554413>
- Gastineau, G, D'Andrea, F and Frankignoul, C.** 2013. Atmospheric response to the north Atlantic ocean variability on seasonal to decadal time scales. *Climate Dynamics*, 40(9): 2311–2330. DOI: <https://doi.org/10.1007/s00382-012-1333-0>
- Granger, C.** 1969. Investigating causal relations by econometric models and cross-spectral methods. *Econometrica*, 37: 424–438. DOI: <https://doi.org/10.2307/1912791>
- Hagan, DFT, Wang, G, Liang, XS and Dolman, HAJ.** 2019. A time-varying causality formalism based on the Liang-Kleeman information flow for analyzing directed interactions in nonstationary climate systems. *Journal of Climate*, 32(21): 7521–7537. DOI: <https://doi.org/10.1175/JCLI-D-18-0881.1>
- Johnson, ZF, Chikamoto, Y, Wang, S-YS, McPhaden, MJ and Mochizuki, T.** 2020. Pacific decadal oscillation remotely forced by the equatorial Pacific and the Atlantic oceans. *Climate Dynamics*, 55: 789–811. DOI: <https://doi.org/10.1007/s00382-020-05295-2>
- Kravtsov, S, Dewar, WK, Berloff, P, McWilliams, JC and Ghil, M.** 2007. A highly nonlinear coupled mode of decadal variability in a mid-latitude ocean-atmosphere model. *Dynamics of Atmospheres and Oceans*, 43(3): 123–150. DOI: <https://doi.org/10.1016/j.dynatmoce.2006.08.001>
- Liang, XS.** 2016. Information flow and causality as rigorous notions ab initio. *Physical Review E*, 94: 052201. DOI: <https://doi.org/10.1103/PhysRevE.94.052201>
- Liang, XS.** 2018. Causation and information flow with respect to relative entropy. *Chaos*, 28: 075311. DOI: <https://doi.org/10.1063/1.5010253>
- Liang, XS and Kleeman, R.** 2005. Information transfer between dynamical system components. *Physical Review Letters*, 95: 244101. DOI: <https://doi.org/10.1103/PhysRevLett.95.244101>
- Liang, XS.** 2014a. Entropy evolution and uncertainty estimation with dynamical systems. *Entropy*, 16(7): 3605–3634. DOI: <https://doi.org/10.3390/e16073605>
- Liang, XS.** 2014b. Unraveling the cause-effect relation between time series. *Phys. Rev. E*, 90: 052150. DOI: <https://doi.org/10.1103/PhysRevE.90.052150>
- Liang, XS.** 2021. Normalized multivariate time series causality analysis and causal graph reconstruction. *Entropy*, 23(6). DOI: <https://doi.org/10.3390/e23060679>
- Lin, H and Derome, J.** 2004. Nonlinearity of the extratropical response to tropical forcing. *Journal of Climate*, 17(13): 2597–2608. DOI: [https://doi.org/10.1175/1520-0442\(2004\)017<2597:NOTERT>2.0.CO;2](https://doi.org/10.1175/1520-0442(2004)017<2597:NOTERT>2.0.CO;2)
- Liu, Z and Alexander, MA.** 2007. Atmospheric bridge, oceanic tunnel, and global climatic teleconnections. *Reviews of Geophysics*, 45: RG2005. DOI: <https://doi.org/10.1029/2005RG000172>
- Mann, ME, Steinman, BA and Miller, SK.** 2014. On forced temperature changes, internal variability, and the AMO. *Geophysical Research Letters*, 41(9): 3211–3219. DOI: <https://doi.org/10.1002/2014GL059233>
- Mantua, NJ, Hare, SR, Zhang, Y, Wallace, JM and Francis, RC.** (1997). A Pacific interdecadal climate oscillation with impacts on salmon production*. *Bulletin of the American Meteorological Society*, 78(6): 1069–1080. DOI: [https://doi.org/10.1175/1520-0477\(1997\)078<1069:APICOW>2.0.CO;2](https://doi.org/10.1175/1520-0477(1997)078<1069:APICOW>2.0.CO;2)
- Merryfield, WJ, Baehr, J, Batt, L, Becker, EJ, Butler, AH, Coelho, CAS, Danabasoglu, G, Dirmeyer, PA, Doblaser-Reyes, FJ, Domeisen, DIV, Ferranti, L, Ilynia, T, Kumar, A, Miller, WA, Rixen, M, Robertson, AW, Smith, DM, Takaya, Y, Tuma, M, Vitart, F, White, CJ, Alvarez, MS, Ardilouze, C, Attard, H, Baggett, C, Balmaseda, MA, Beraki, AF, Bhattacharjee, PS, Bilbao, R, de Andrade, FM, DeFlorio, MJ, Daz, LB, Ehsan, MA, Fragkoulidis, G, Grainger, S, Green, BW, Hell, MC, Infantini, JM, Isensee, K, Kataoka, T, Kirtman, BP, Klingaman, NP, Lee, J-Y, Mayer, K, McKay, R, Mecking, JV, Miller, DE, Neddermann, N, Ng, CHJ, Oss, A, Pankatz, K, Peatman, S, Pegion, K, Perlwitz, J, Recalde-Coronel, GC, Reintges, A, Renkl, C, Solaraju-Murali, B, Spring, A, Stan, C, Sun, YQ, Tozer, CR, Vigaud, N, Woolnough, S and Yeager, S.** 2020. Current and emerging developments in subseasonal to decadal prediction. *Bulletin of the American Meteorological Society*, 101(6): E869–E896. DOI: <https://doi.org/10.1175/BAMS-D-19-0037.1>
- Mokhov, I and Smirnov, D.** 2006. Study of the mutual influence of the El-Niño-southern oscillation processes and the north Atlantic and Arctic oscillations. *Izvestiya, Atmospheric and Oceanic Physics*, 42: 650–667. DOI: <https://doi.org/10.1134/S0001433806050069>
- Mosedale, TJ, Stephenson, DB, Collins, M and Mills, TC.** 2006. Granger causality of coupled climate processes: Ocean feedback on the north Atlantic oscillation. *Journal of Climate*, 19(7): 1182–1194. DOI: <https://doi.org/10.1175/JCLI3653.1>
- Newman, M, Alexander, MA, Ault, TR, Cobb, KM, Deser, C, Lorenzo, ED, Mantua, NJ, Miller, AJ, Minobe, S, Nakamura, H, Schneider, N, Vimont, DJ, Phillips, AS, Scott, JD and Smith, CA.** 2016. The Pacific decadal

- oscillation, revisited. *Journal of Climate*, 29(12): 4399–4427. DOI: <https://doi.org/10.1175/JCLI-D-15-0508.1>
- Newman, M, Compo, GP and Alexander, A.** 2003. Enso-forced variability of the Pacific decadal oscillation. *Journal of Climate*, 16(23): 3853–3857. DOI: [https://doi.org/10.1175/1520-0442\(2003\)016<3853:EVOTPD>2.0.CO;2](https://doi.org/10.1175/1520-0442(2003)016<3853:EVOTPD>2.0.CO;2)
- Nicolis, C and Nicolis, G.** 1995. From short-scale atmospheric variability to global climate dynamics: Toward a systematic theory of averaging. *Journal of the Atmospheric Sciences*, 52(11): 1903–1913. DOI: [https://doi.org/10.1175/1520-0469\(1995\)052<1903:FSSAVT>2.0.CO;2](https://doi.org/10.1175/1520-0469(1995)052<1903:FSSAVT>2.0.CO;2)
- Nicolis, C and Nicolis, G.** 1998. Closing the hierarchy of moment equations in nonlinear dynamical systems. *Physical Review E*, 58(4): 4391–4400. DOI: <https://doi.org/10.1103/PhysRevE.58.4391>
- Nigam, S, Sengupta, A and Ruiz-Barradas, A.** 2020. Atlantic-pacific links in observed multidecadal SST variability: Is the atlantic multidecadal oscillation's phase reversal orchestrated by the pacific decadal oscillation? *Journal of Climate*, 33(13): 5479–5505. DOI: <https://doi.org/10.1175/JCLI-D-19-0880.1>
- Palus, M, Krakovská, A, Jakubík, J and Chvosteková, M.** 2018. Causality, dynamical systems and the arrow of time. *Chaos: An Interdisciplinary Journal of Nonlinear Science*, 28(7): 075307. DOI: <https://doi.org/10.1063/1.5019944>
- Pegion, K, Kirtman, BP, Becker, E, Collins, DC, LaJoie, E, Burgman, R, Bell, R, DelSole, T, Min, D, Zhu, Y, Li, W, Sinsky, E, Guan, H, Gottschalck, J, Metzger, EJ, Barton, NP, Achuthavari, D, Marshak, J, Koster, RD, Lin, H, Gagnon, N, Bell, M, Tippett, MK, Robertson, AW, Sun, S, Benjamin, SG, Green, BW, Bleck, R and Kim, H.** 2019. The subseasonal experiment (SUBX): A multimodel subseasonal prediction experiment. *Bulletin of the American Meteorological Society*, 100(10): 2043–2060. DOI: <https://doi.org/10.1175/BAMS-D-18-0270.1>
- Philander, SGH.** 1990. *El-Niño, La Niña, and the Southern Oscillation*, volume 46 of *International Geophysics*. San Diego: Academic Press.
- Roads, JO.** 1987. Predictability in the extended range. *Journal of Atmospheric Sciences*, 44(23): 3495–3527. DOI: [https://doi.org/10.1175/1520-0469\(1987\)044<3495:PI TER>2.0.CO;2](https://doi.org/10.1175/1520-0469(1987)044<3495:PI TER>2.0.CO;2)
- Runge, J, Bathiany, S, Bollt, E, Camps-Valls, G, Coumou, D, Deyle, E, Glymour, C, Kretschmer, M, Mahecha, MD, Muoz-Mar, J, van Nes, EH, Peters, J, Quax, R, Reichstein, M, Scheffer, M, Schlkopf, B, Spirtes, P, Sugihara, G, Sun, J, Zhang, K and Zscheischler, J.** 2019. Inferring causation from time series in earth system sciences. *Nature Communications*, 10(1): 2553. DOI: <https://doi.org/10.1038/s41467-019-10105-3>
- Saltzman, B.** 1983. Climate systems analysis. *Advances in Geophysics*, 25: 173–233. DOI: [https://doi.org/10.1016/S0065-2687\(08\)60174-0](https://doi.org/10.1016/S0065-2687(08)60174-0)
- Soulard, N, Lin, H, Derome, J and Yu, B.** 2021. Tropical forcing of the circumglobal teleconnection pattern in boreal winter. *Climate Dynamics*, 57: 865–877. DOI: <https://doi.org/10.1007/s00382-021-05744-6>
- Stan, C, Straus, DM, Frederiksen, JS, Lin, H, Maloney, ED and Schumacher, C.** 2017. Review of tropical-extratropical teleconnections on intraseasonal time scales. *Reviews of Geophysics*, 55(4): 902–937. DOI: <https://doi.org/10.1002/2016RG000538>
- Thompson, DWJ and Wallace, JM.** 1998. The Arctic oscillation signature in the wintertime geopotential height and temperature fields. *Geophysical Research Letters*, 25(9): 1297–1300. DOI: <https://doi.org/10.1029/98GL00950>
- Tsonis, AA, Deyle, ER, May, RM, Sugihara, G, Swanson, K, Verbeten, JD and Wang, G.** 2015. Dynamical evidence for causality between galactic cosmic rays and interannual variation in global temperature. *Proceedings of the National Academy of Sciences*, 112(11): 3253–3256. DOI: <https://doi.org/10.1073/pnas.1420291112>
- Tsonis, AA and Swanson, KL.** 2012. Review article “on the origins of decadal climate variability: A network perspective”. *Nonlinear Processes in Geophysics*, 19(5): 559–568. DOI: <https://doi.org/10.5194/npg-19-559-2012>
- Vannitsem, S, Dalaiden, Q and Goosse, H.** 2019. Testing for dynamical dependence: Application to the surface mass balance over Antarctica. *Geophysical Research Letters*, 46(21): 12125–12135. DOI: <https://doi.org/10.1029/2019GL084329>
- Vannitsem, S and Ekelmans, P.** 2018. Causal dependences between the coupled ocean-atmosphere dynamics over the tropical Pacific, the north Pacific and the north Atlantic. *Earth System Dynamics*, 9(3): 1063–1083. DOI: <https://doi.org/10.5194/esd-9-1063-2018>
- Vannitsem, S and Ghil, M.** 2017. Evidence of coupling in ocean-atmosphere dynamics over the north Atlantic. *Geophys. Res. Lett.*, 44(4): 2016–2026. DOI: <https://doi.org/10.1002/2016GL072229>
- Vannitsem, S and Nicolis, C.** 1998. Dynamics of fine-scale variables versus averaged observables in a t21l3 quasi-geostrophic model. *Quarterly Journal of the Royal Meteorological Society*, 124(551): 2201–2226. DOI: <https://doi.org/10.1002/qj.49712455103>
- Wallace, JM and Gutzler, DS.** 1981. Teleconnections in the geopotential height field during the northern hemisphere winter. *Monthly Weather Review*, 109(4): 784–812. DOI: [https://doi.org/10.1175/1520-0493\(1981\)109<0784:TITGH F>2.0.CO;2](https://doi.org/10.1175/1520-0493(1981)109<0784:TITGH F>2.0.CO;2)
- Wang, G, Swanson, KL and Tsonis, AA.** 2009. The pacemaker of major climate shifts. *Geophysical Research Letters*, 36(7): L07708. DOI: <https://doi.org/10.1029/2008GL036874>
- Wang, J, Kim, H-M and Chang, EKM.** 2017. Changes in northern hemisphere winter storm tracks under the background of Arctic amplification. *Journal of Climate*, 30(10): 3705–3724. DOI: <https://doi.org/10.1175/JCLI-D-16-0650.1>
- Yang, J, Chen, H, Song, Y, Zhu, S, Zhou, B and Zhang, J.** 2021. Atmospheric circumglobal teleconnection triggered by spring land thermal anomalies over west Asia and its possible impacts on early summer climate over northern China. *Journal of Climate*, 34(14): 5999–6021. DOI: <https://doi.org/10.1175/JCLI-D-20-0911.1>

TO CITE THIS ARTICLE:

Vannitsem, S and Liang, XS. 2022. Dynamical Dependencies at Monthly and Interannual Time Scales in the Climate System: Study of the North Pacific and Atlantic Regions. *Tellus A: Dynamic Meteorology and Oceanography*, 74(2022), 141–158. DOI: <https://doi.org/10.16993/tellusa.44>

Submitted: 28 September 2021 Accepted: 24 February 2022 Published: 29 March 2022

COPYRIGHT:

© 2022 The Author(s). This is an open-access article distributed under the terms of the Creative Commons Attribution 4.0 International License (CC-BY 4.0), which permits unrestricted use, distribution, and reproduction in any medium, provided the original author and source are credited. See <http://creativecommons.org/licenses/by/4.0/>.

Tellus A: Dynamic Meteorology and Oceanography is a peer-reviewed open access journal published by Stockholm University Press.

